

## RITA Mimics: Synthesis and Mechanistic Evaluation of Asymmetric Linked Trithiazoles

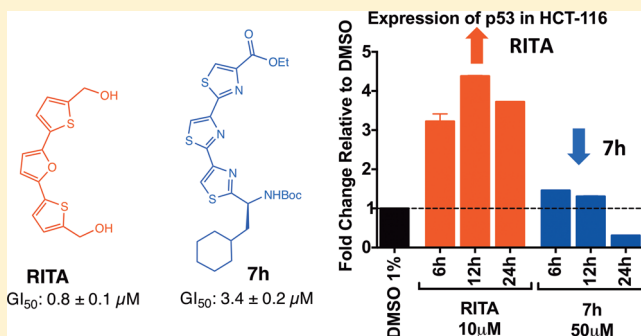
Adrian L. Pietkiewicz,<sup>†</sup> Yuqi Zhang,<sup>†</sup> Marwa N. Rahimi, Michael Stramandinoli, Matthew Teusner, and Shelli R. McAlpine\*<sup>✉</sup>

School of Chemistry, University of New South Wales, Sydney, NSW 2052, Australia

## Supporting Information

**ABSTRACT:** The established cytotoxic agent RITA contains a thiophene–furan–thiophene backbone and two terminal alcohol groups. Herein we investigate the effect of using thiazoles as the backbone in RITA-like molecules and modifying the terminal groups of these trithiazoles, thereby generating 41 unique structures. Incorporating side chains with varied steric bulk allowed us to investigate how size and a stereocenter impacted biological activity. Subjecting compounds to growth inhibition assays on HCT-116 cells showed that the most potent compounds **7d**, **7e**, and **7h** had  $GI_{50}$  values of 4.4, 4.4, and 3.4  $\mu\text{M}$ , respectively, versus RITA ( $GI_{50}$  of 800 nM). Analysis of these compounds in apoptosis assays proved that **7d**, **7e**, and **7h** were as effective as RITA at inducing apoptosis. Evaluating the impact of **7h** on proteins targeted by RITA (p53, c-Myc, and Mcl-1) indicated that it acts via a different mechanism of action to that of RITA. RITA suppressed Mcl-1 protein via p53, whereas compound **7h** suppressed Mcl-1 expression via an alternative mechanism independent of p53.

**KEYWORDS:** Heterocycle, RITA, thiazole, antitumor, Mcl-1, p53, c-Myc



Heterocycles comprise one of the largest compound classes of all known molecules. Over 10 million heterocyclic scaffolds have been identified since 2000.<sup>1</sup> Linked azole moieties are present in many bioactive compounds,<sup>2–5</sup> and substituting a thiazole into the molecular backbone can improve the biological activity of a molecule over other heterocyclic substitutions.<sup>6–8</sup> Thiazole-containing compounds have efficacy as antibacterial,<sup>9</sup> anticonvulsive,<sup>10</sup> antifungal,<sup>11</sup> antiviral,<sup>12</sup> and anticancer<sup>13,14</sup> agents. One successful thiazole drug, dasatinib (Sprycel), was FDA-approved as a chronic myeloid leukemia (CML) chemotherapeutic (Figure 1a).<sup>15</sup> LCL-161 (Figure 1b) is currently in Phase II clinical trials, where it is being assessed to treat myelofibrosis.<sup>16</sup>

Thiazoles provide rigidity to the compound's structure compared to alkyl or peptide moieties from which they are generated, which leads to lower entropic costs upon binding to a target compared to molecules with the same atoms that are not locked into a ring system. Thiazoles also offer  $\pi$ -stacking opportunities with protein targets.<sup>17,18</sup> In contrast to thiazoles, similar structures containing oxazoles and triazoles can be significantly less active, in some cases by greater than 10-fold than those containing thiazoles.<sup>6–8,19,20</sup>

Molecules containing three 2,4-linked thiazoles and an ester or amide functional group at one end (structures 1–3, Figure 1c) are cytotoxic against the human colorectal carcinoma cell line HCT-116.<sup>6,7</sup> Similar structures where thiazoles in 1–3 were replaced with oxazoles were completely inactive.<sup>6,7</sup> The 2,4-linked heterocyclic scaffold present in molecules 1, 2, and 3

is also present in NSC 652287 (RITA) (Figure 1c),<sup>21</sup> which contains a 2,4-linked thiophene–furan–thiophene backbone and terminal alcohol groups.<sup>21</sup> RITA is of significant biological interest as a cytotoxic agent because it interferes with the p53–HDM-2 interaction, a key oncogenic binding event.<sup>22</sup> Inhibiting binding between HDM-2 and p53 activates p53, which subsequently induces apoptosis. RITA also suppresses expression of numerous oncogenic proteins including Mcl-1 and c-Myc, which also promote apoptosis.<sup>23</sup> Recent studies involving CRISPR-Cas9-mediated gene disruption have also shown that RITA is cytotoxic in cells deficient in p53.<sup>24</sup> Cells resistant to RITA could be made RITA-sensitive when FancD2 or mTor proteins were inhibited.<sup>24</sup> These results indicate that RITA is biologically active even in the absence of p53 protein.

Elegant work by Wipf and co-workers describes a series of linked thiophenes and furans that had similar structures and activity to RITA (4–5 Figure 1c).<sup>20</sup> Research by Jiang and co-workers also showed that a linked trithiophene **6** has cytotoxic potency.<sup>25</sup> The primary alcohols on RITA, and structures 4–6 were essential to the molecules' biological activity. Jiang et al.<sup>25</sup> showed that replacing one of the thiophene groups with a furan to form a thiophene-difuran diol lead to a loss in cytotoxic activity by almost 10-fold. The linked trifuran species lead to a complete loss in cytotoxic activity of the diol, suggesting that

Received: December 1, 2016

Accepted: March 6, 2017

Published: March 6, 2017



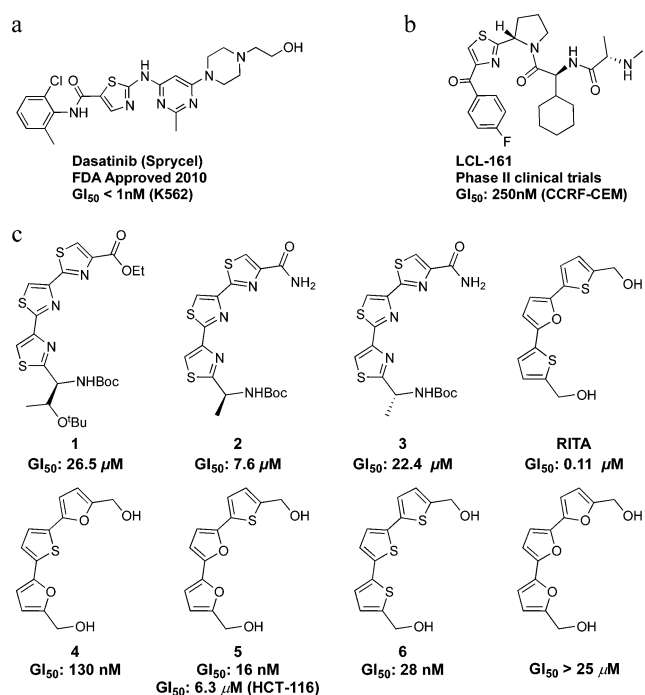


**Figure 1.** (a) Thiazole-containing chemotherapeutic drug approved by the FDA. (b) Thiazole-containing compound in clinical trials. (c) Trithiazoles 1–3<sup>6,7,20</sup> and RITA<sup>20</sup> with their reported activity against HCT-116 colon cancer cell line, 4–5 generated from Wipf lab,<sup>20</sup> and 6 from Gao and Jiang lab against MCF-7 breast cancer line.<sup>25</sup>

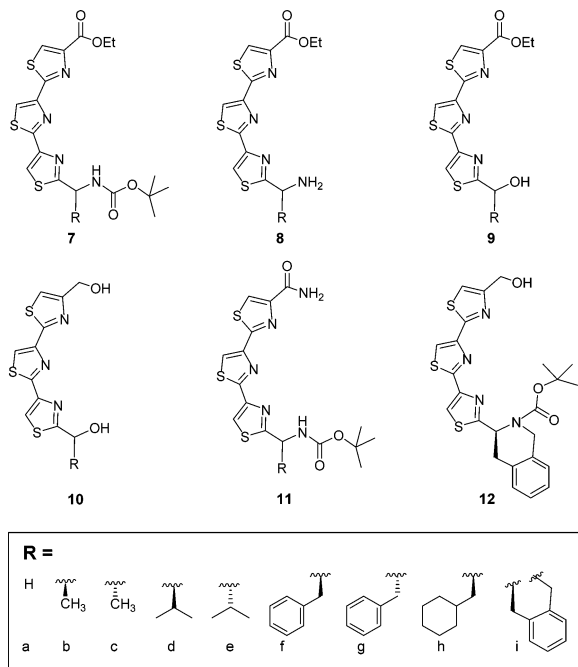
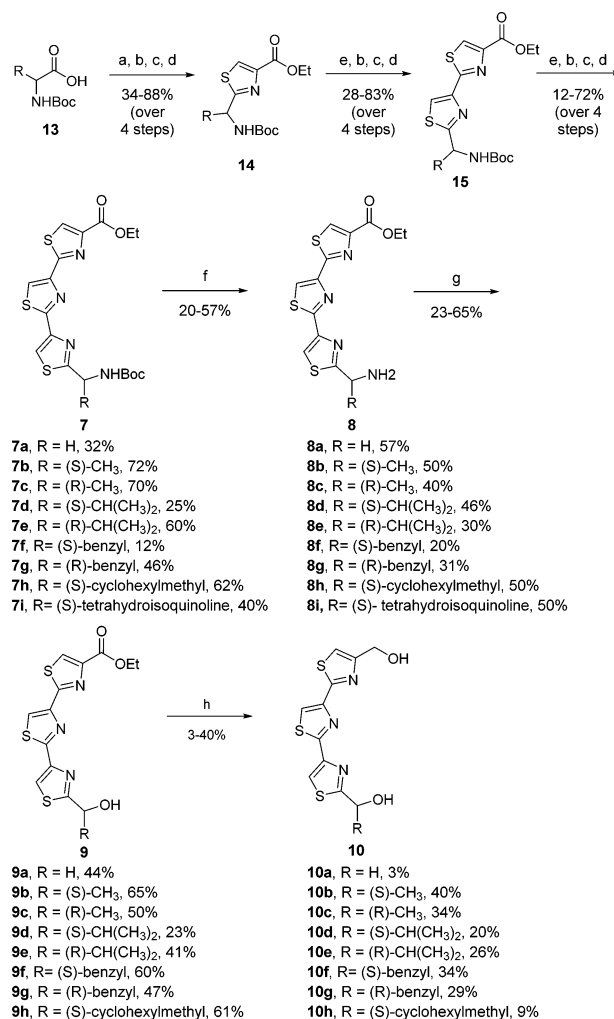


**Figure 2.** Structures of 7a–i, 8a–i, 9a–h, 10a–h, 11a–h, and 12.

the thiophene moieties, and particularly the sulfur group, are important for cytotoxic activity. Computational studies have shown that thiazoles have a larger aromatic character compared to furans, and behave similarly to thiophenes,<sup>26</sup> which may explain Jiang's results. By increasing the aromatic character in the molecular backbone, there is increased potential for the compound to undergo  $\pi$ -stacking with target proteins. Incorporating thiazole moieties into the compound can also

### Scheme 1. Synthesis of Trithiazole Analogue Series 7–10<sup>a</sup>



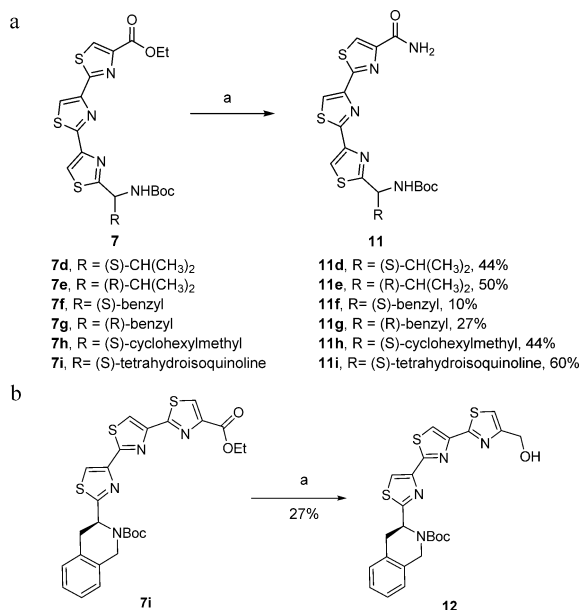
<sup>a</sup>Reagents and conditions: (a) BOP, DIPEA, NH<sub>4</sub>OH, CH<sub>2</sub>Cl<sub>2</sub>, N<sub>2</sub>, rt, 16 h. (b) Lawesson's reagent, benzene/THF, 60 °C/rt, 6 h. (c) KHCO<sub>3</sub>, ethyl bromopyruvate, DME, rt, 16 h. (d) Py, TFAA, TEA, DME, 0 °C–rt, 7 h. (e) NH<sub>4</sub>OH, MeOH, rt, 14 h. (f) TFA, anisole, CH<sub>2</sub>Cl<sub>2</sub>, rt, 1 h. (g) NaNO<sub>2</sub>, H<sub>2</sub>SO<sub>4</sub>, 1,4-dioxane, 0 °C–rt, 14 h. (h) LiAlH<sub>4</sub>, THF, N<sub>2</sub>, 0 °C–rt, 2 h.

increase compound hydrophilicity via H-bonding with the nitrogen atom in the ring.<sup>27</sup>

Structures 7a–i, which are similar to 1 in that they contain an ester and amine with a *tert*-butyloxy carbonyl (Boc) protecting group, were synthesized with methyl (7b, 7c), isopropyl (7d, 7e), benzyl (7f, 7g), (S)-cyclohexylmethyl (7h), and (S)-tetrahydroisoquinoline (7i) at position R. These side chains were chosen to evaluate the effect of biological activity as the steric bulk of the side chain increased. Removal of the Boc group produced series 8a–i. Conversion of the amine in each structure to an alcohol generated molecules 9a–h. Reduction of the ester to the alcohol produced diol compounds labeled as 10a–h. Conversion of the ester 7 to the amide gave molecules labeled as 11a–h. An (S)-tetrahydroisoquinoline analogue 12 was also synthesized, containing Boc and alcohol groups.

With the goal of understanding how thiazoles impact the biological activity and the relevance of the alcohol group compared to other moieties, we synthesized and mechanistically evaluated series 7–11 (Figure 2). These series were hybrid structures of 1–3 and 4–6, thereby allowing us to

## Scheme 2. Syntheses of Trithiazole Analogues 11d–i and 12



investigate how the trithiazole and primary alcohol contributed to the compound's overall activity. Mechanistic studies including cytotoxicity against HCT-116 colon cancer cell lines, apoptosis induction, and impact on expression of p53, Mcl-1, and *c-Myc* are also described for the three most active molecules.

Syntheses of structures **7a–i** were based on the synthetic strategy developed by Islam and co-workers (Scheme 1).<sup>7</sup>

Starting from the appropriate Boc-protected amino acid **13**, thiazole **14** was produced via reaction with ammonia in the presence of (benzotriazol-1-yloxy) tris(dimethylamino)phosphonium hexafluorophosphate (BOP), *N,N*-diisopropylethylamine (DIPEA), and ammonium hydroxide to form the corresponding amide. The amide was then reacted with Lawesson's reagent to yield the thioamide. The thioamide was condensed with ethyl bromopyruvate and KHCO<sub>3</sub> and subsequently dehydrated using trifluoroacetic acid anhydride (TFAA) in the presence of pyridine (Py) and quenched with triethylamine (TEA), employing a modified Hantzsch synthesis to form the monothiazole (34–88% yield). Series **14** were converted to the dithiazoles **15** by converting the monothiazole ester to the amide using ammonium hydroxide and then repeating the thioamidation and modified Hantzsch synthesis (yields 28–83% over 4 steps). Conversion of the dithiazole into trithiazole structures **7a–i** was accomplished by amidation, thioamidation, and modified Hantzsch synthesis to yield compounds **7a–i** (12–72% yield).

The compound series **7a–i** was reacted with trifluoroacetic acid (TFA) to produce compounds **8a–i** (yields 20–57%). The series **9a–h** was synthesized by reacting **8a–h** with sodium nitrite in concentrated sulfuric acid and 1,4-dioxane (23–65% yield). The diol series **10a–h** was synthesized by reducing compounds **9a–h** with LiAlH<sub>4</sub> (3–40% yield).

Compound **11a** was not generated, and compounds **11b–c** have been previously reported<sup>7</sup> and have no biological activity. Series **11d–i** were produced by converting analogues **7d–i** to their corresponding amide via sonication in ammonium

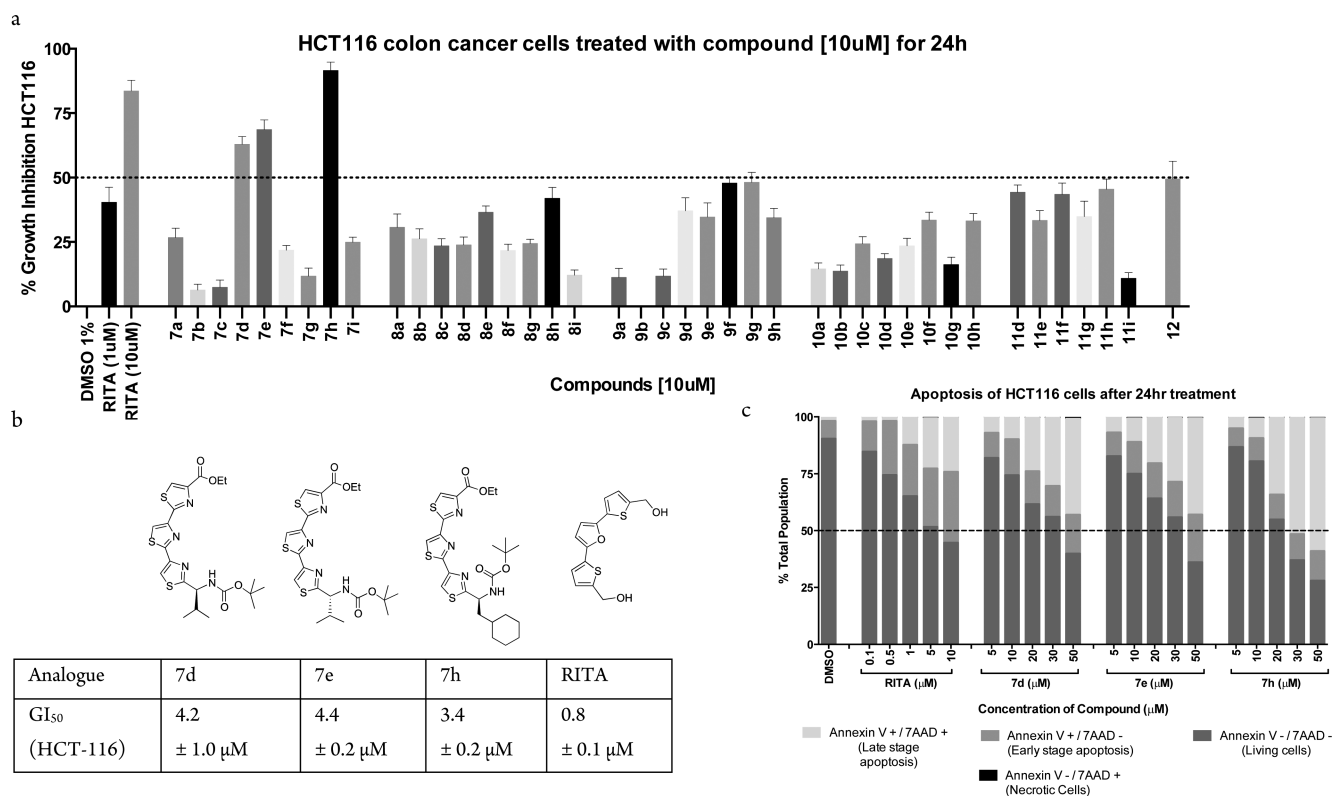


**Figure 3.** (a) Growth inhibition assay on trithiazole analogues at 10 μM of compound over 24 h against HCT-116 cells. (b) GI<sub>50</sub> values of most cytotoxic analogues (see Supporting Information for growth inhibition curves). (c) Apoptosis induction caused by RITA, **7d**, **7e**, and **7h** at 24 h in HCT116 cells. All values shown are the average ± SEM from at least three independent experiments.

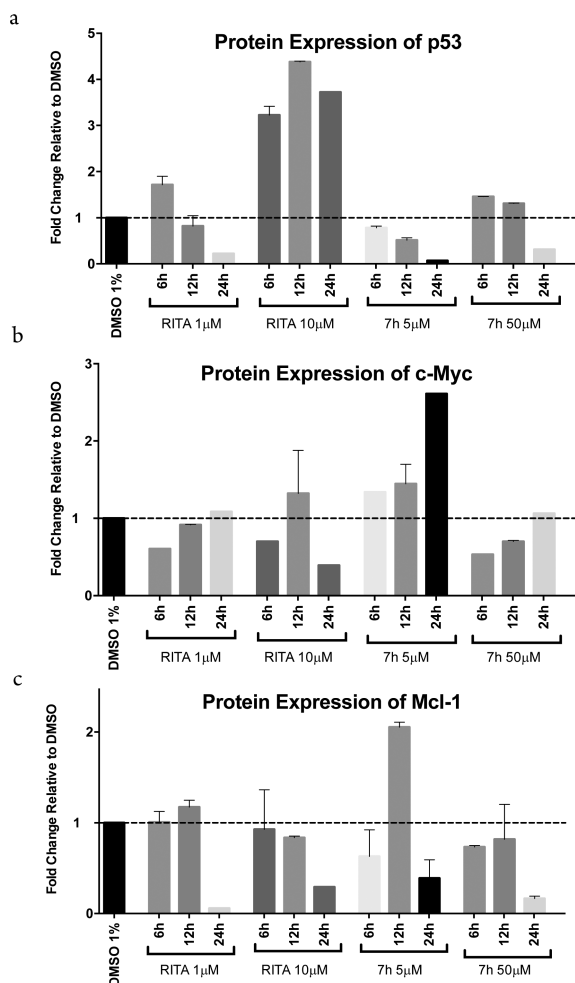


**Figure 4.** (a) Expression level of p53 at 6, 12, and 24 h against HCT-116 cells following treatment with DMSO (1%), RITA (1  $\mu$ M), and 7h (5  $\mu$ M, 50  $\mu$ M). (b) Expression levels of *c-Myc* at 6, 12, and 24 h against HCT-116 cells following treatment with DMSO (1%), RITA (1  $\mu$ M, 10  $\mu$ M), and 7h (5  $\mu$ M, 50  $\mu$ M). (c) Expression level of Mcl-1 at 6, 12, and 24 h against HCT-116 cells following treatment with DMSO (1%), RITA (1  $\mu$ M, 10  $\mu$ M), and 7h (5  $\mu$ M, 50  $\mu$ M).

hydroxide (Scheme 2a, yields 10–60%). The (S)-tetrahydroisoquinoline analogue **12** was synthesized by  $\text{LiAlH}_4$  reduction of **7i** in THF (27% yield, Scheme 2b).

Upon completing the compound synthesis all molecules were tested for their ability to inhibit growth when colon cancer HCT-116 cell line was treated with compounds at a concentration of 10  $\mu$ M for 24 h (Figure 3a). DMSO was a negative control, and RITA was a positive control. Of the ester series, **7d**, **7e**, and **7h** were found to be the most potent analogues, showing between 50 and 100% growth inhibition. Surprisingly, no analogues in series **8**, **9**, **10**, or **11** showed significant cytotoxic activity despite structural similarities to RITA.

The lack of cytotoxic activity in series **10** was surprising, as this series most closely resembled the lead structures, suggesting that the thiophene ring in RITA is important for biological activity. Comparing **10a** and RITA, we see the sulfur groups of **10a** are in a different position than in RITA. The thiophene ring in RITA also contains a hydrophobic HC–CH bond opposite the heteroatoms, whereas the thiazoles in **10a**

contain a heteroatom on the ring and the alkyl bond is absent. This alkyl bond appears to play a key role in the cytotoxicity of RITA given that there is a difference between RITA and **10a**.

After the initial growth inhibition screening, the most potent analogues, **7d**, **7e**, and **7h**, were tested for their  $\text{GI}_{50}$ : **7d** ( $4.4 \pm 1.0 \mu\text{M}$ ), **7e** ( $4.4 \pm 0.2 \mu\text{M}$ ), and **7h** ( $3.4 \pm 0.2 \mu\text{M}$ ) (Figure 3b). Thus, the triazole esters with aliphatic bulky side chains were the most promising leads. Despite being similar in size to the side chains on the active molecules the benzyl and tetrahydroisoquinoline (TIC) analogues (**7e**, **7f**, and **7i**, respectively) were not nearly as active as those with isopropyl and cyclohexylmethyl side chains (**7d**, **7e**, and **7h**).

Apoptosis assays were evaluated on the three most active compounds (**7d**, **7e**, and **7h**) and run based on their  $\text{GI}_{50}$  values in HCT-116 cells (Figure 3c). An initial concentration of 5  $\mu$ M was chosen for compounds **7d**, **7e**, and **7h** as this concentration was just above each compound's  $\text{GI}_{50}$  value and would be easy for others to replicate. Comparing 1  $\mu$ M RITA to 5  $\mu$ M **7d**, **7e**, and **7h** showed that RITA induced apoptosis more effectively than **7d**, **7e**, and **7h**. However, treating cells with 10-fold over the  $\text{GI}_{50}$  concentration (10  $\mu$ M RITA versus 50  $\mu$ M **7d**, **7e**, and **7h**) showed that **7d** and **7e** were slightly more effective and that **7h** was almost 2-fold more effective at inducing apoptosis than RITA.

We investigated the mechanism by which **7h**, our most effective molecule, induced apoptosis and compared it to RITA's mechanism for impacting p53 protein levels in the cell. It is established that RITA activates p53, inducing expression of this antiapoptotic protein. The current belief is that through activation of p53, RITA suppresses the expression of numerous oncogenic proteins including Mcl-1 and *c-Myc*.<sup>21–23</sup> Thus, we evaluated the expression levels of p53, *c-Myc*, and Mcl-1 when HCT116 cells were treated with RITA and **7h**. The impact of RITA on protein levels are usually monitored over time rather than varying the concentration of the compound in order to observe the initial increase and then decrease of p53 at a single concentration of RITA. The levels of p53 are then correlated to a decrease in *c-Myc* and Mcl-1. Thus, we investigated changes in p53, *c-Myc*, and Mcl-1 over time but also over concentration (Figure 4a–c).

Treating HCT116 cells with 1  $\mu$ M RITA produced an increase in p53 at 6 h. A peak in p53 protein levels was seen at 12 h when treating with 10  $\mu$ M (~10-fold over the  $\text{GI}_{50}$ ). In contrast, treating cells with **7h** did not produce an increase in p53, rather p53 decreased with treatment time. Evaluating *c-Myc* after treatment with 1  $\mu$ M RITA over time showed that initially *c-Myc* protein decreased relative to control, but then returned to normal levels. The 10  $\mu$ M *c-Myc* treatment, however, produced an intense decrease in *c-Myc* protein expression. This trend is similar to data produced by others, where *c-Myc* decreases as p53 levels are increased. Monitoring *c-Myc* upon treatment of **7h** showed an increase in the protein after 5  $\mu$ M treatment and 24 h. These data correlate to the levels of p53, which decreased by 10-fold after 24 h of 5  $\mu$ M treatment. Treatment with **7h** at 50  $\mu$ M produces the same trend as treatment at 5  $\mu$ M, where there is a decrease in p53 levels, which likely produces an increase in *c-Myc* levels.

Examining Mcl-1 protein levels after treatment with RITA and **7h** showed that both concentrations of RITA and **7h** produced a drop in Mcl-1 protein over time (almost 10-fold). Levels of Mcl-1 are known to drop when treated with RITA because they are regulated by the increase in p53. However, treatment with **7h** does not increase p53; therefore, the

expression levels of Mcl-1 do not correlate to p53 expression levels. Thus, in contrast to RITA, where an increase in p53 is linked to a decrease in Mcl-1, **7h** produces a decrease in p53, but also a decrease in Mcl-1. Treating cells with **7h** produces almost a 10-fold decrease in the Mcl-1 protein (Figure 4c, 24 h, 50  $\mu$ M). This interesting phenomenon suggests that a protein other than p53 is regulating the decrease of Mcl-1. In conclusion, we have synthesized 41 compounds that were based on the structure of RITA. These compounds were tested for their ability to kill HCT-116 cells, induce apoptosis, and regulate p53 and oncogenic proteins *c-Myc* and Mcl-1. As reported by others, RITA induces p53 protein and decreases the level of both oncogenic proteins. Our most potent compound **7h** has a slightly higher  $GI_{50}$  than RITA and induces apoptosis at similar levels to RITA. Yet **7h** acts via a mechanism that is distinct from that of RITA. It does not induce high levels of p53, yet it increases the protein levels of *c-Myc* and decreases the protein levels of Mcl-1 in cancer cells. This behavior is distinct from the p53 inducing compound RITA and, as such, provides an interesting tool for suppressing Mcl-1 protein levels via an alternative mechanism.

## ■ ASSOCIATED CONTENT

### Supporting Information

The Supporting Information is available free of charge on the ACS Publications website at DOI: 10.1021/acsmedchemlett.6b00488.

Experimental procedures and all spectra collected during the synthesis (PDF)

## ■ AUTHOR INFORMATION

### Corresponding Author

\*E-mail: s.mcalpine@unsw.edu.au. Tel: +61 4 1672-8896.

### ORCID

Shelli R. McAlpine: 0000-0003-1058-5252

### Author Contributions

<sup>†</sup>These authors contributed equally to the manuscript. A.L.P. synthesized “series f, g, and h” and created the first draft of the manuscript. Y.Z. synthesized “series b, c, e, i, and 12” and collated the Supporting Information. M.N.R. ran the biological assays. M.S. synthesized “series a”. M.T. synthesized “series d”. S.R.M. conceived of the project, assisted in experimental design and interpretation, and heavily edited the final version of the manuscript.

### Funding

The University of New South Wales, School of Chemistry supported this research.

### Notes

The authors declare no competing financial interest.

## ■ ACKNOWLEDGMENTS

We thank the School of Chemistry at the University of New South Wales for providing funding for this project. A.L.P. and M.N.R. thank the Australian government for providing an APA scholarship. We thank the staff of Mark Wainwright Analytical Centre.

## ■ ABBREVIATIONS

BOP, (benzotriazol-1-yloxy)tris(dimethylamino)phosphonium hexafluorophosphate; DIPEA, *N,N*-diisopropylethylamine; DME, 1,2-dimethoxyethane; TFAA, trifluoroacetic acid anhy-

dride; Py, pyridine; TEA, triethylamine; TFA, trifluoroacetic acid

## ■ REFERENCES

- (1) Dua, R.; Shrivastava, S.; Sonwane, S. K.; Srivastava, S. K. Pharmacological Significance of Synthetic Heterocycles Scaffold: A Review. *Adv. Biol. Res.* **2011**, *5*, 120–144.
- (2) Riego, E.; Hernández, D.; Albericio, F.; Álvarez, M. Directly Linked Polyazoles: Important Moieties in Natural Products. *Synthesis* **2005**, *2005*, 1907–1922.
- (3) Duchler, M. G-quadruplexes: targets and tools in anticancer drug design. *J. Drug Target.* **2012**, *20*, 389–400.
- (4) Dang, Q.; Yan, L.; Cashion, D. K.; Kasibhatla, S. R.; Jiang, T.; Taplin, F.; Jacintho, J. D.; Li, H.; Sun, Z.; Fan, Y.; DaRe, J.; Tian, F.; Li, W.; Gibson, T.; Lemus, R.; van Poelje, P. D.; Potter, S. C.; Erion, M. D. Discovery of a series of phosphonic acid-containing thiazoles and orally bioavailable diamide prodrugs that lower glucose in diabetic animals through inhibition of Fructose-1,6-bisphosphatase. *J. Med. Chem.* **2011**, *54*, 153–165.
- (5) Rzuczek, S. G.; Pilch, D. S.; Liu, A.; LaVoie, E. J.; Rice, J. E. Macrocyclic pyridyl polyoxazoles: selective RNA and DNA G-quadruplex ligands as antitumor agents. *J. Med. Chem.* **2010**, *53*, 3632–3644.
- (6) Kim, S.-J.; Lin, C.-C.; Pan, C.-M.; Ranaware, D. P.; Ramsey, D. M.; McAlpine, S. R. A structure-activity relationship study on multi-heterocyclic molecules: two linked thiazoles are required for cytotoxic activity. *MedChemComm* **2013**, *4*, 406–410.
- (7) Islam, A.; Zhang, Y.; Wang, Y.; McAlpine, S. R. Design, synthesis, and anticancer activity of linked azoles. *MedChemComm* **2015**, *6*, 300–305.
- (8) Pan, C.-M.; Lin, C.-C.; Kim, S. J.; Sellers, R. P.; McAlpine, S. R. Progress toward the synthesis of Urukthapelstatin A and two analogues. *Tetrahedron Lett.* **2012**, *53*, 4065–4069.
- (9) Darwish, E.; Fattah, A.; Attaby, F.; Al-Shayea, O. Synthesis and Antimicrobial Evaluation of Some Novel Thiazole, Pyridone, Pyrazole, Chromene, Hydrazone Derivatives Bearing a Biologically Active Sulfonamide Moiety. *Int. J. Mol. Sci.* **2014**, *15*, 1237.
- (10) Hays, S. J.; Rice, M. J.; Ortwine, D. F.; Johnson, G.; Schwarz, R. D.; Boyd, D. K.; Copeland, L. F.; Vartanian, M. G.; Boxer, P. A. Substituted 2-benzothiazolamines as sodium flux inhibitors: Quantitative structure–activity relationships and anticonvulsant activity. *J. Pharm. Sci.* **1994**, *83*, 1425–1432.
- (11) Maillard, L. T.; Bertout, S.; Quinonéro, O.; Akalin, G.; Turan-Zitouni, G.; Fulcrand, P.; Demirci, F.; Martinez, J.; Masurier, N. Synthesis and anti-Candida activity of novel 2-hydrazino-1,3-thiazole derivatives. *Bioorg. Med. Chem. Lett.* **2013**, *23*, 1803–1807.
- (12) Paget, C. J.; Kisner, K.; Stone, R. L.; DeLong, D. C. Heterocyclic substituted ureas. II. Immunosuppressive and antiviral activity of benzothiazolyl- and benzoxazolylureas. *J. Med. Chem.* **1969**, *12*, 1016–1018.
- (13) Das, J.; Moquin, R. V.; Lin, J.; Liu, C.; Doweyko, A. M.; DeFex, H. F.; Fang, Q.; Pang, S.; Pitt, S.; Shen, D. R.; Schieven, G. L.; Barrish, J. C.; Wityak, J. Discovery of 2-amino-heteroaryl-benzothiazole-6-anilides as potent p53 inhibitors. *Bioorg. Med. Chem. Lett.* **2003**, *13*, 2587–2590.
- (14) Hutchinson, I.; Bradshaw, T. D.; Matthews, C. S.; Stevens, M. F. G.; Westwell, A. D. Antitumour benzothiazoles. Part 20:  $\ddagger$  3'-Cyano and 3'-Alkynyl-Substituted 2-(4'-Aminophenyl)benzothiazoles as new potent and selective analogues. *Bioorg. Med. Chem. Lett.* **2003**, *13*, 471–474.
- (15) Breccia, M.; Stagno, F.; Luciano, L.; Abruzzese, E.; Annunziata, M.; D'Adda, M.; Maggi, A.; Sgherza, N.; Russo-Rossi, A.; Pregno, P.; Castagnetti, F.; Iurlo, A.; Latagliata, R.; Cedrone, M.; Di Renzo, N.; Sorà, F.; Rege-Cambrin, G.; La Nasa, G.; Scortechini, A. R.; Greco, G.; Franceschini, L.; Sica, S.; Bocchia, M.; Crugnola, M.; Orlandi, E.; Guarini, A.; Specchia, G.; Rosti, G.; Saglio, G.; Alimena, G. Dasatinib first-line: Multicentric Italian experience outside clinical trials. *Leuk. Res.* **2016**, *40*, 24–29.

- (16) Mullard, A. Pioneering apoptosis-targeted cancer drug poised for FDA approval. *Nat. Rev. Drug Discovery* **2016**, *15*, 147–149.
- (17) Gomtsyan, A. Heterocycles in drugs and drug discovery. *Chem. Heterocycl. Compd.* **2012**, *48*, 7–10.
- (18) Huber, R. G.; Margreiter, M. A.; Fuchs, J. E.; von Grafenstein, S.; Tautermann, C. S.; Liedl, K. R.; Fox, T. Heteroaromatic  $\pi$ -Stacking Energy Landscapes. *J. Chem. Inf. Model.* **2014**, *54*, 1371.
- (19) Davis, M. R.; Singh, E. K.; Wahyudi, H.; Alexander, L. D.; Kunicki, J.; Nazarova, L. A.; Fairweather, K. A.; Giltrap, A. M.; Jolliffe, K. A.; McAlpine, S. R. Synthesis of Sansalvamide A peptidomimetics: Trizazole, Oxazole, Thiazole, and Pseudoproline containing compounds. *Tetrahedron* **2012**, *68*, 1029–1051.
- (20) Salamoun, J.; Anderson, S.; Burnett, J. C.; Gussio, R.; Wipf, P. Synthesis of heterocyclic triads by Pd-Catalyzed Cross-couplings and evaluation of their cell-specific toxicity profile. *Org. Lett.* **2014**, *16*, 2034–2037.
- (21) Rivera, M. I.; Stinson, S. F.; Vistica, D. T.; Jorden, J. L.; Kenney, S.; Sausville, E. A. Selective toxicity of the tricyclic thiophene NSC 652287 in renal carcinoma cell lines: Differential accumulation and metabolism. *Biochem. Pharmacol.* **1999**, *57*, 1283–1295.
- (22) Issaeva, N.; Bozko, P.; Enge, M.; Protopopova, M.; Verhoef, L. G. G. C.; Masucci, M.; Pramanik, A.; Selivanova, G. Small molecule RITA binds to p53, blocks p53-HDM2 interaction and activates p53 function in tumors. *Nat. Med.* **2004**, *10*, 1321–1328.
- (23) Grinkevich, V. V.; Nikulenkov, F.; Shi, Y.; Enge, M.; Bao, W.; Maljukova, A.; Gluch, A.; Kel, A.; Sangfelt, O.; Selivanova, G. Ablation of Key Oncogenic Pathways by RITA-Reactivated p53 Is Required for Efficient Apoptosis. *Cancer Cell* **2009**, *15*, 441–453. *Cancer Cell* **2009**, *15*, 441–453.
- (24) Wanzel, M.; Vischedyk, J. B.; Gittler, M. P.; Gremke, N.; Seiz, J. R.; Hefter, M.; Noack, M.; Savai, R.; Mernberger, M.; Charles, J. P.; Schneikert, J.; Bretz, A. C.; Nist, A.; Stiewe, T. CRISPR-Cas9-based target validation for p53-reactivating model compounds. *Nat. Chem. Biol.* **2016**, *12*, 22–28.
- (25) Lin, J.; Jin, X.; Bu, Y.; Cao, D.; Zhang, N.; Li, S.; Sun, Q.; Tan, C.; Gao, C.; Jiang, Y. Efficient synthesis of RITA and its analogues: derivation of analogues with improved antiproliferative activity via modulation of p53/miR-34a pathway. *Org. Biomol. Chem.* **2012**, *10*, 9734–9746.
- (26) Horner, K. E.; Karadakov, P. B. Shielding in and around Oxazole, Imidazole, and Thiazole: How Does the Second Heteroatom Affect Aromaticity and Bonding? *J. Org. Chem.* **2015**, *80*, 7150–7157.
- (27) Prezhdo, O. V.; Lysova, I. V.; Distanov, V. B.; Prezhdo, V. V. Synthesis and scintillating efficiencies of 2,5-diarylthiazoles with intramolecular hydrogen bond. *Tetrahedron Lett.* **2004**, *45*, 5291.